

Visualization of Flow Regimes in Symmetric Microchannel in Case of Different Inlet Flowrate Ratios for Fixed Outlet Reynolds Number

A. Yu. Kravtsova*

*Kutateladze Institute of Thermophysics, Siberian Branch, Russian Academy of Sciences,
Novosibirsk, Russia*

Received April 22, 2020; in final form, October 12, 2020; accepted October 23, 2020

Abstract—An experimental investigation of flow pattern regimes and mixing inside a T-type microchannel for different inlet flowrate ratios was carried out. Seven flow pattern regimes were obtained experimentally. Partial penetration of the flow into the opposite input channel with occurrence of one vortex was shown by Rahimi et al. [8]. We experimentally demonstrate arising of two vortex structures rotating about their axes in the case of partial penetration of the flow into the opposite input channel. In addition, we reveal appearance of periodic waviness streaks, absent in previous works. We also investigated the evolution of a transparent periodic vortex structure inside the outlet microchannel. It is a very slow periodic process. The mixing efficiency for all flow regimes is estimated. A maximum mixing of 0.87 is achieved for the streaks and unsteady regimes. We also discover that the biggest mixing efficiency is equal to 0.67, reached at $R = 0.25$ and a low outlet Reynolds number $Re = 47$.

DOI: 10.1134/S1810232820040098

1. INTRODUCTION

Compact devices such as micro-electromechanical systems, micromixers, microreactors, and portable electronic devices implemented using the concept of fuel cell are based on microchannels as part of their design. Compactness of microchannels together with a high surface-to-volume ratio enhances the fluid mixing. Changing the flowrate ratio has been proposed as a method of enhancing mixing in microfluidic channels (Poole et al. [7]). Poole et al. [7] investigated the transition from a steady flow to unsteady one for various flowrate ratios inside a T-microchannel. They used numerical simulation to show that the change in the flow structure depends on the bifurcation parameter, defined as the maximum value of spanwise velocity on the bifurcation line.

Chakraborty et al. [2] investigated the flow in T-shaped micromixers on rotating platforms. They identified three regimes of mixing based on different flow behaviors in each of these regimes. A diffusion-based mixing regime was obtained for low rotation speeds. A mixing regime based on the Coriolis force was observed for intermediate rotation speeds. An instability-based mixing regime was discovered at very high rotational speeds. This regime is characterized by a streak flow pattern, which allows a significant increase in the efficiency of flow mixing.

Ansari et al. [1] analyzed a vortex flow in a T-mixer with non-aligned inputs. The mixer generates formation of mixing-inducing flows even at low Reynolds numbers as compared with a simple T-mixer. The vortex initially formed at the inlet of rectangular microchannel increases the interfacial area of the fluid streams due to stretching. Vortices in the form of streak flow in the outlet channel were observed experimentally. An increase in the mixing efficiency was observed.

Rahimi et al. [8] investigated the effect of channel confluence angle, flowrate, and flowrate ratio on the mixing performance in a passive mixing test. The mixing effectiveness grows with increase in the flowrate ratio and decrease in the confluence angle. They demonstrated that the mixing performance depends on the channel geometry, total flowrate, and inlet flowrate ratios. They showed only four regime flows

*E-mail: Kravtsova.Alya@gmail.com

occurring in channels. The aim of our paper is demonstration of experimental visualized flow pattern structures inside a symmetric T-microchannel in the case of different inlet flowrate ratios for various outlet Reynolds numbers and the effect of flow regimes on the mixing efficiency.

2. MEASUREMENT TECHNIQUE

An experimental investigation of flow pattern regimes and mixing in the case of different ratios of inlet flowrates in a T-shaped microchannel has been carried out. The T-microchannel was made of optically transparent material SU-8 with dimensions of $120 \times 120 \times 240 \mu\text{m}$ (height H , input channel width W_{in} , and output channel width W_{out}). The flowrates were varied from 0.39 ml/h to 202 ml/h in each of the inlet channels (Fig. 1). The Reynolds number was obtained for the mixing channel using its characteristic hydraulic diameter D_h and mean flow velocity U_0 ; ν was the kinematic viscosity of the flow, the value of which was taken for room temperature and was defined as $\text{Re} = U_0 \cdot D_h / \nu$. The hydraulic diameter of the outlet channel $D_h = 4 \cdot S_{\text{out}} / P_{\text{out}}$, where $S_{\text{out}} = H \cdot W_{\text{out}}$ and $P_{\text{out}} = 2(H + W_{\text{out}})$ are the cross-section area and perimeter of the mixing channel, correspondingly, was $160 \mu\text{m}$.

The Reynolds number in the outlet channel varied from 3 to 560. The mixing process in the microchannel was achieved by changing the inlet flowrate ratios. Since the geometry of the T-microchannel was symmetric, we assumed that the inlet left flowrate was less than the inlet right flowrate, $Q_1 < Q_2$. The inlet flowrate ratio was defined as the coefficient $R = Q_1 / Q_2$, where the flowrate Q_1 was obtained for the left inlet channel and the flowrate Q_2 was obtained for the right channel. The

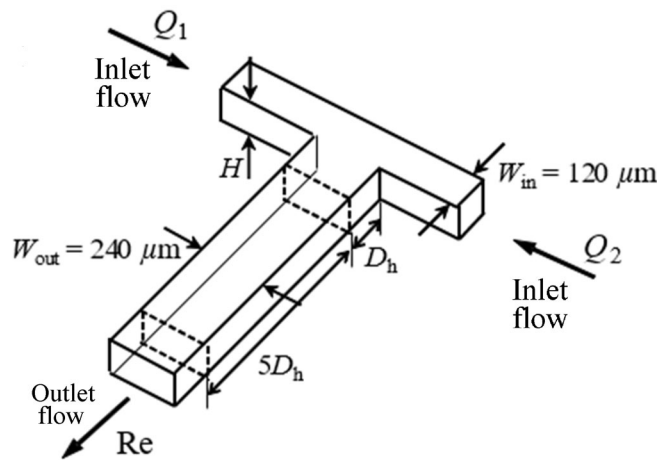


Fig. 1. Scheme of experimental working channel.

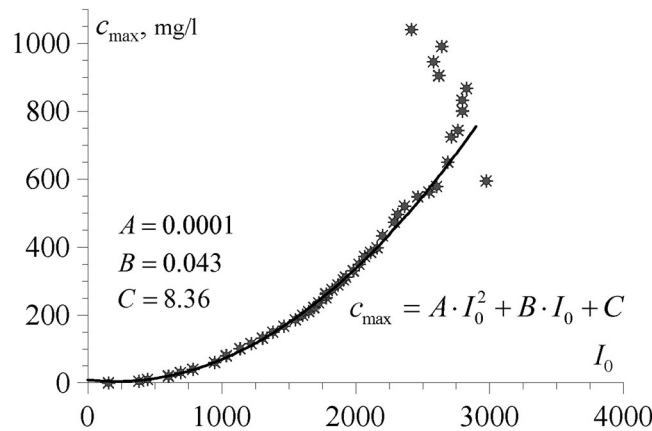


Fig. 2. Average image brightness I_0 against concentration of solution Rhodamine 6G with liquid c_{max} .

values of so-determined R were always less or equal to 1. To visualize the flow pattern regimes, the laser induced fluorescence (LIF) method was applied (its description is given in Kravtsova et al. [5]). The concentration of solution was 362 mg/l.

To calculate the quantitative parameters of mixing based on concentration fields, a calibration curve was constructed. For each concentration value, 100 images were taken. The next step was averaging the obtained images. The resulting set of averaged images at various concentrations of solution and distilled water in the stream was used to plot the concentration as a function of brightness at the image point. The calibration curve was supplemented with correction factors for each image point, intended to eliminate the effect of inhomogeneous illumination of flow and obtained by averaging the ratio of the average image brightness to the brightness at a point over all calibration images (see Fig. 2). The calibration curve was approximated with a polynomial function of second degree for Rhodamine 6G solution. Then we restored the concentration field from instantaneous images of the stream according to the calibration (Sakakibara et al. [9, 10]).

Using the instantaneous concentration fields, the concentration profiles in each cross-section channel were constructed and the mixing efficiency was estimated using the intensive segregation by

Dankwerts [3]: $I_M = 1 - \sigma/\sigma_0$, where $\sigma^2 = \frac{1}{N} \sum_{i=1}^N (c_i - \bar{c})^2$, \bar{c} is the average value of concentration, $\sigma_0^2 = \bar{c}(c_{\max} - \bar{c})$ is the maximum root mean square deviation for mixing the liquid with a concentration of 0 and c_{\max} , where c_{\max} is the maximum concentration of the Rhodamine 6G dye. Thus, the liquids are completely mixed at $I_M = 1$ and segregated at $I_M = 0$.

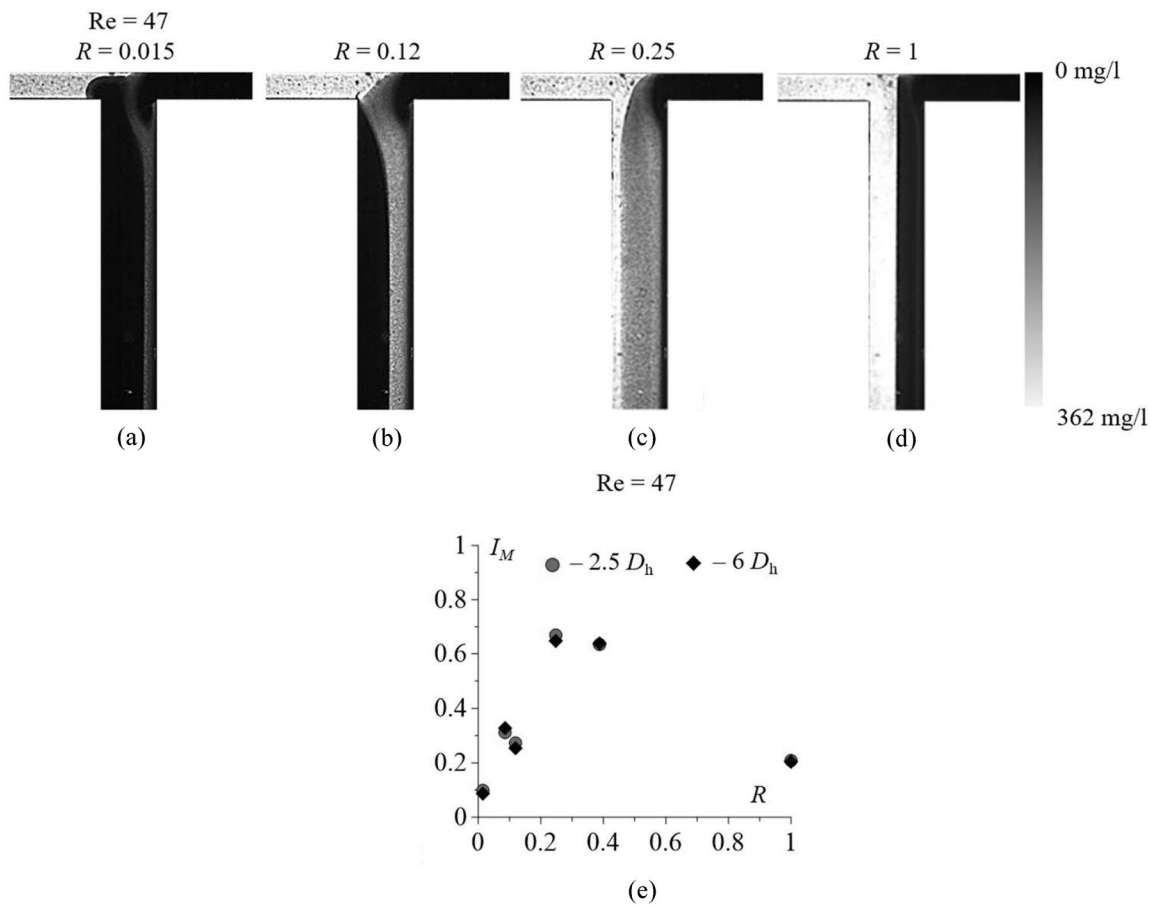


Fig. 3. Effect of different ratios of inlet flowrates on flow pattern regimes in T-shaped microchannel at $Re = 47$: (a) $R = 0.015$, (b) $R = 0.12$, (c) $R = 0.25$, (d) $R = 1$, and (e) mixing efficiency.

3. RESULTS

Instantaneous concentration fields showing the flow structure in the experimental channel are presented in Figs. 3–6. The left inlet flow is pale grey; the right inlet flow is black. The grayscale distribution in the images illustrates the features of the flow structure and enables mixing intensity calculation.

Partial penetration of the flow into the opposite input channel was obtained for the inlet flowrate ratio $R = 0.015$ (Fig. 3a). Rahimi et al. [8] used numerical simulation to show occurrence of one vortex structure in the inlet channel in this place. We detected that the edge between the liquids shifted along the inlet channel slightly. The shift was less than $3 \mu\text{m}$. At the same time, some part of the left flow penetrated into the outlet channel and streamed along the right wall. The flow stream width colored pale grey in the figure is $0.2W_{\text{out}}$. The flow structure changed for the flowrate ratio $R = 0.12$ (Fig. 3b). The flow width inside the outlet channel grew up to $0.4W_{\text{out}}$. The flow was stationary. A significant change in the microflow structure took place for the flowrate ratio $R = 0.25$ (Fig. 3c). Thin bands of flows of the same color as the input liquids run along the nearest walls of the outlet channel. In Fig. 3c, however, the wide gray band is observed in the central part of the channel.

The transition from pale grey to black became the smoothest across the channel. Since diffusive mixing is proportional to the concentration gradient, the outlet flow featured intensified mixing (see Fig. 3e). The evident homogeneity of this outlet flow was determined by the high mixing intensity of the flows as compared with other regimes shown in Fig. 3. The mixing efficiency was 0.67. Thus, based on this comparison we can conclude that the inlet flowrate variation has much potential to intensify the mixing of fluids inside microchannels. At the same time, with equal input streams (Fig. 3d), the flows in

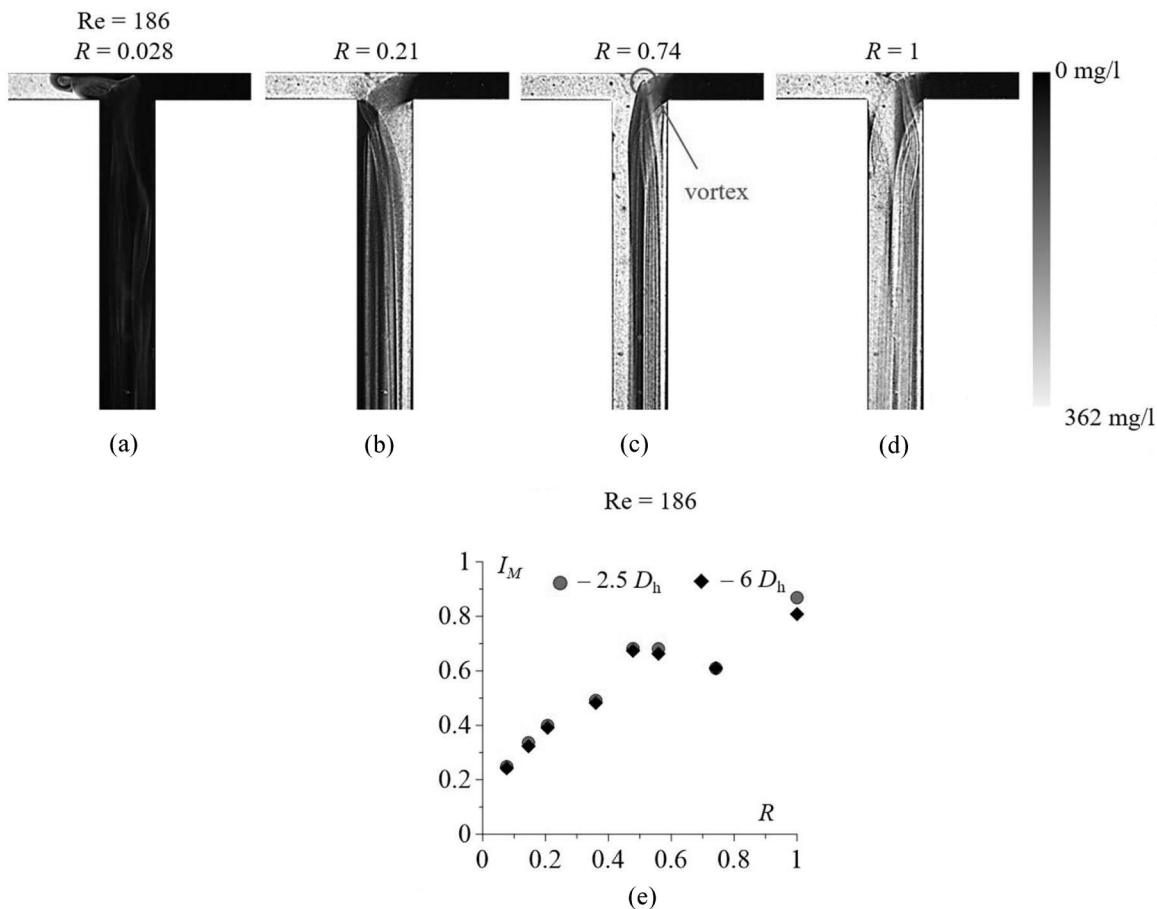


Fig. 4. Effect of different ratios of inlet flowrates on flow pattern regimes in T-shaped microchannel at $\text{Re} = 186$: (a) $R = 0.028$, (b) $R = 0.21$, (c) $R = 0.74$, (d) $R = 1$, and (e) mixing efficiency.

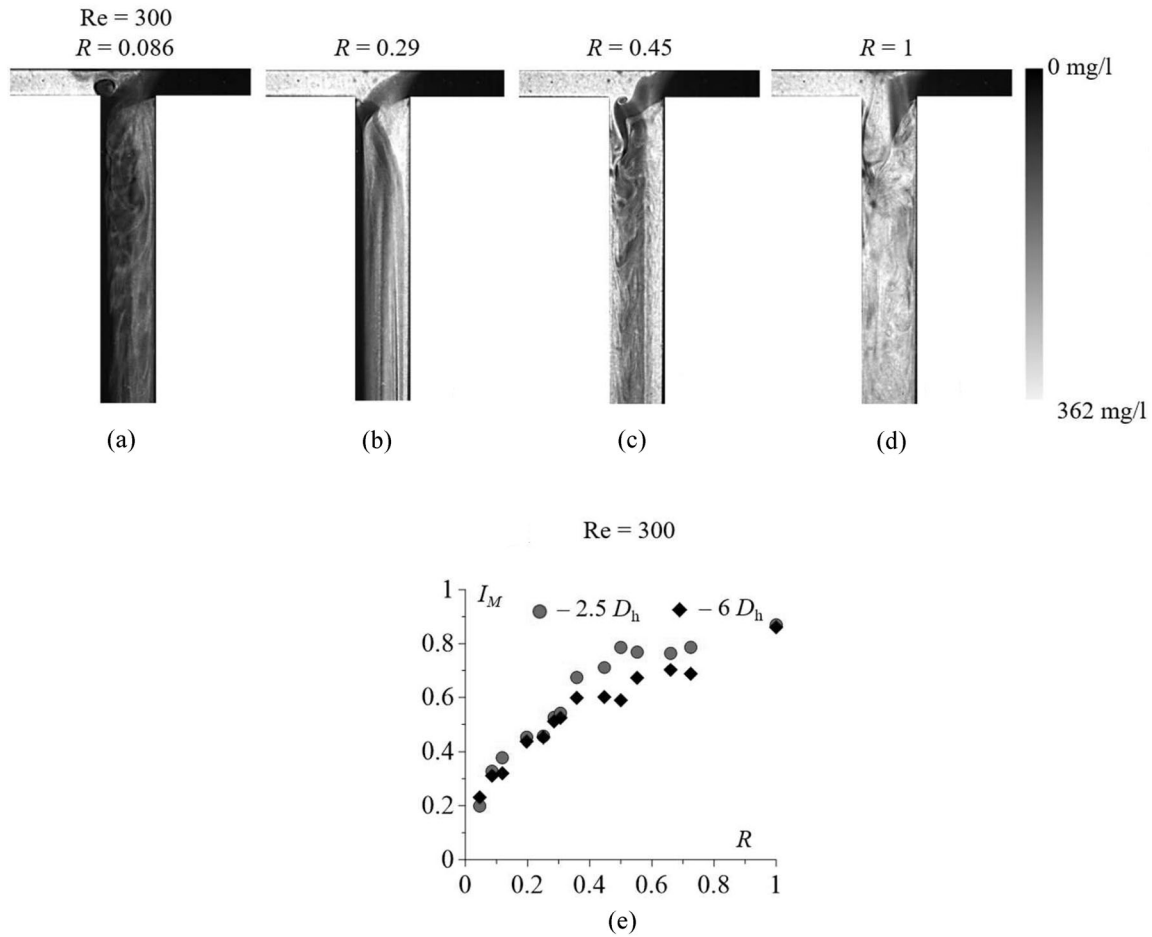


Fig. 5. Effect of different ratios of inlet flowrates on flow pattern regimes in T-shaped microchannel at $Re = 300$: (a) $R = 0.086$, (b) $R = 0.29$, (c) $R = 0.45$, (d) $R = 1$, and (e) mixing efficiency.

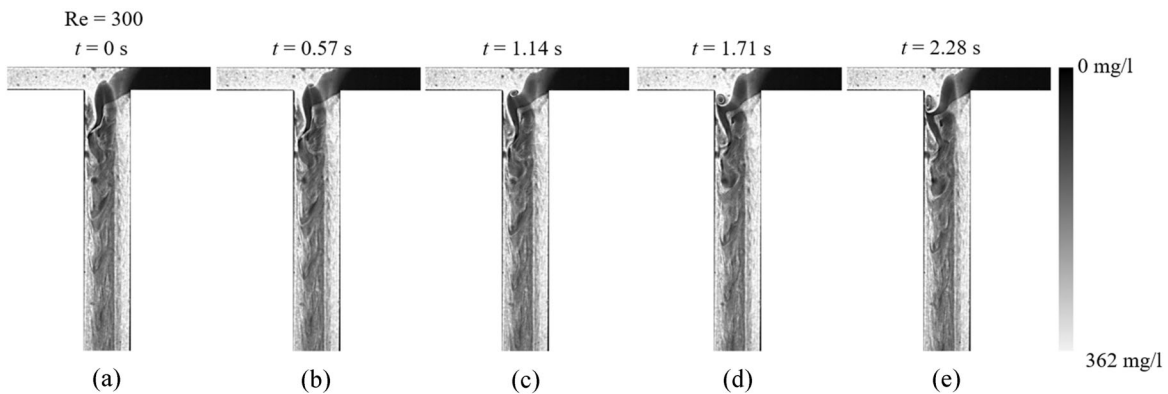


Fig. 6. Evolution of transparent periodic vortex structure for $Re = 300$ and $R = 0.45$.

the output channel touched each other along the thin contact line and, as a result, no effective mixing occurred (Fig. 3e). The mixing efficiency was about 0.21.

The flow pattern regimes appearing at different flowrate ratios for a fixed outlet Reynolds number $Re = 186$ are shown in Fig. 4. Two vortex structures occurred in the case of partial penetration of the right flow into the opposite input channel for the inlet flowrate ratio $R = 0.028$ (Fig. 4a). The vortices rotated about their axes and had opposite directions of rotation, which caused unsteadiness of the flow in the output

channel. At a flowrate ratio of 0.21, 0.74, and 1 and an outlet Reynolds number of 186, streaks appeared inside the outlet channel (Figs. 4b–4d). The flow inside the outlet channel was stationary. A description of this regimes is given by Chakraborty et al. [2]. Increase in the number of layers between the flows caused growth of the mixing efficiency. It is demonstrated in Fig. 4e. The maximum mixing efficiency was equal to 0.87 for the engulfment regime with $R = 1$, as described by Fani et al. [4], Mariotti et al. [6], and others. Besides, we observed formation of a small vortex at the junction of inlet flows due to their partial engulfment by each other at $R = 0.74$ (Fig. 4c).

Partial penetration of the flow into the opposite input channel with formation of a rotating vortex structure and additional partial inflow of liquid is shown in Fig. 5a. Rotation of the vortex in the input channel entailed occurrence of unsteadiness in the output channel. The flow structure visualized in Fig. 5b is similar to the flow pattern regimes for $Re = 186$ and $R = 0.21$. However, this regime is transitional between stationary streaks and unsteady flow. The appearance of periodic waviness streaks is characteristic of this regime. The mixing efficiency was 0.52 (Fig. 5e). An interesting flow regime was obtained in the case of $Re = 300$ with the input ratio $R = 0.45$ (Fig. 5c). The occurrence of a transverse vortex structure, which determines the flow structure in the output channel, was examined (see Fig. 6). For $Re = 300$ and $R = 1$, the flow structure was defined as an unsteady periodic asymmetric regime and features of this structure were demonstrated by Mariotti et al. [6]. The maximum mixing efficiency was 0.87 for $R = 1$.

Formation of a small vortex due to partial engulfment of the left flows in the central part of the channel is presented in Fig. 6a. In 0.57 sec, the vortex left the confluence region and shifted to the opposite half of the outlet channel due to the effect of the quicker right inlet flow. The size of the vortex grew (Figs. 6b–6d). The vortex rotated across the outlet channel. Since the flow velocity at the near walls was less than that in the center part of the channel, the vortex flattened and elongated while travelling downstream. The bottom halves of the outlets show the dissipated vortices to be reminiscent of the wave structures spreading along the left wall of the channel in Fig. 6e. This process was periodic.

Thus, we visualized seven flow pattern regimes inside a symmetric microchannel in the case of different inlet flowrate ratios. A maximum mixing of 0.87 was achieved at streaks and unsteady regimes. We discovered that the biggest mixing efficiency was equal to 0.7 and was reached at $R = 0.25$ and a low outlet Reynolds number $Re = 47$.

FUNDING

The work was supported by the Russian Science Foundation (project no. 19-79-10217).

REFERENCES

1. Ansari, M.A., Kim, K.Y., Anwar, K., and Kim, S.M., Vortex Micro T-Mixer with Non-Aligned Inputs, *Chem. Engin. J.*, 2012, vols. 181/182, pp. 846–850.
2. Chakraborty, D., Madoub, M., and Chakraborty, S., Anomalous Mixing Behaviour in Rotationally Actuated Microfluidic Devices, *Lab Chip.*, 2011, vol. 11, pp. 2823–2826.
3. Dankwerts, P.V., The Definition and Measurements of Some Characteristics of Mixtures, *Appl. Sci. Res.*, 1958, pp. 279–296.
4. Fani, A., Camarri, S., and Salvetti, M.V., Investigation of the Steady Engulfment Regime in a Three-Dimensional T-Mixer, *Phys. Fluids*, 2013, vol. 25, p. (064102)-17.
5. Kravtsova, A.Yu., Ianko, P.E., Kashkarova, M.V., and Bilsky, A.V., Investigation of the Perturbation Flow in a T-Microchannel Using the LIF Technique, *J. Visual.*, 2019, vol. 22, no. 5, pp. 851–855.
6. Mariotti, A., Galletti, C., Mauri, R., Salvetti, M.V., and Brunazzi, E., Steady and Unsteady Regimes in a T-Shaped Micro-Mixer: Synergic Experimental and Numerical Investigation, *Chem. Engin. J.*, 2018, vol. 341, pp. 414–431.
7. Poole, R.J., Alfateh, M., and Gauntlett, A.P., Bifurcation in a T-Channel Junction: Effects of Aspect Ratio and Shear-Thinning, *Chem. Engin. Sci.*, 2013, vol. 104, pp. 839–848.
8. Rahimi, M., Akbari, M., Parsamoghadam, M., and Alsairafi, A., CFD Study on Effect of Channel Confluence Angle on Fluid Flow Pattern in Asymmetrical Shaped Microchannels, *Computers Chem. Engin.*, 2015, vol. 73, pp. 172–182.
9. Sakakibara, J., and Adrian, R.J., Measurements of Temperature Field of a Rayleigh–Benard Convection Using Two-Color Laser-Induced Fluorescence, *Exp. Fluids*, 2004, vol. 37, pp. 331–340.
10. Sakakibara, J., Hishida, K., and Maeda, M., Measurements of Thermally Stratified Pipe Flow Using Image-Processing Techniques, *Exp. Fluids*, 1993, vol. 16, pp. 82–96.